

Evidence of chemical reactions in the hydroxyapatite laser ablation plume with a water atmosphere

P. Serra^{a)} and J. L. Morenza

Universitat de Barcelona, Departament de Física Aplicada i Optica, Avda. Diagonal 647, E-08028 Barcelona, Spain

(Received 11 August 1998; accepted for publication 18 December 1998)

The expansion dynamics of the ablation plume generated by KrF laser irradiation of hydroxyapatite targets in a 0.1 mbar water atmosphere has been studied by fast intensified charge coupled device imaging with the aid of optical bandpass filters. The aim of the filters is to isolate the emission of a single species, which allows separate analysis of its expansion. Images obtained without a filter revealed two emissive components in the plume, which expand at different velocities for delay times of up to 1.1 μ s. The dynamics of the first component is similar to that of a spherical shock wave, whereas the second component, smaller than the first, expands at constant velocity. Images obtained through a 520 nm filter show that the luminous intensity distribution and evolution of emissive atomic calcium is almost identical to those of the first component of the total emission and that there is no contribution from this species to the emission from the second component of the plume. The analysis through a 780 nm filter reveals that atomic oxygen partially diffuses into the water atmosphere and that there is a contribution from this species to the emission from the second component. The last species studied here, calcium oxide, was analyzed by means of a 600 nm filter. The images revealed an intensity pattern more complex than those from the atomic species. Calcium oxide also contributes to the emission from the second component. Finally, all the experiments were repeated in a Ne atmosphere. Comparison of the images revealed chemical reactions between the first component of the plume and the water atmosphere. © 1999 American Institute of Physics. [S0021-8979(99)06906-6]

I. INTRODUCTION

Hydroxyapatite (HA) thin films are suitable bioactive coatings for Ti implants in medical applications. Pulsed laser ablation is an appropriate deposition technique due to the complex stoichiometry of HA. Results as obtained indicate that an atmosphere containing water is needed in order to grow films with good properties,¹⁻⁷ and although several gas mixtures have been tested, we have demonstrated that 100% water is suitable.⁶ This motivated us to undertake a detailed study of HA laser ablation process in order to obtain deeper knowledge of the phenomena involved and to optimize the deposition conditions. Therefore, a complete analysis was developed under high vacuum conditions⁸⁻¹¹ in order to characterize the process in the plainest environment. The study was then extended to a water atmosphere^{8,12} in similar conditions to those normally used in the deposition experiments. In all cases the analyses were carried out through the characterization of the light emitted by the laser generated plume by means of fast intensified charge coupled device (CCD) imaging and optical emission spectroscopy. These allowed us to describe the dynamics and composition of the plume in vacuum and in a water atmosphere. In the former case, the distribution of the emissive species along the plasma was also analyzed with the aid of interferential filters in the collection of the images with the CCD camera.⁹⁻¹¹

Here we use interferential bandpass filters to analyze the distribution of emissive species along the plume in a water atmosphere. The scope of this study is not only to discover the different dynamic behavior of the diverse species in the plume, but also to investigate the presence of chemical reactions with the water atmosphere.

II. EXPERIMENT

A KrF excimer laser beam (Lambda Physik LPX 205i, 248 nm wavelength, 30 ns pulse duration) was focused at an incident angle of 45° through a 500 mm focal length Suprasil lens onto a HA target, leading to a fluence of 2.6 J/cm². The laser beam was partially intercepted by a mask in order to improve the uniformity of the laser spot, which was 0.8 mm high and 3.1 mm wide. The target was a 1.7 g/cm³ pellet made from HA powder pressed at 200 MPa. The experiments were carried out in a high vacuum chamber evacuated first by a turbomolecular pump to a base pressure of 5 × 10⁻⁵ mbar and then filled with water vapor at 0.1 mbar.

Images of the ablation plume were taken in single-shot mode with a gated CCD camera (ANIMATER-VI from ARP France) 288 × 385 pixels, 8 bits dynamic range, intensified by a microchannel plate (MCP), whose aperture was delayed by a pulse generator that also triggered the laser shot. The variable MCP gain was set just short of saturation for each image, which gave the maximum intensity resolution. In addition, three bandpass filters (10 nm full width at half maximum) centered at 520, 600, and 780 nm were placed be-

^{a)}Electronic mail: pserra@fao.ub.es

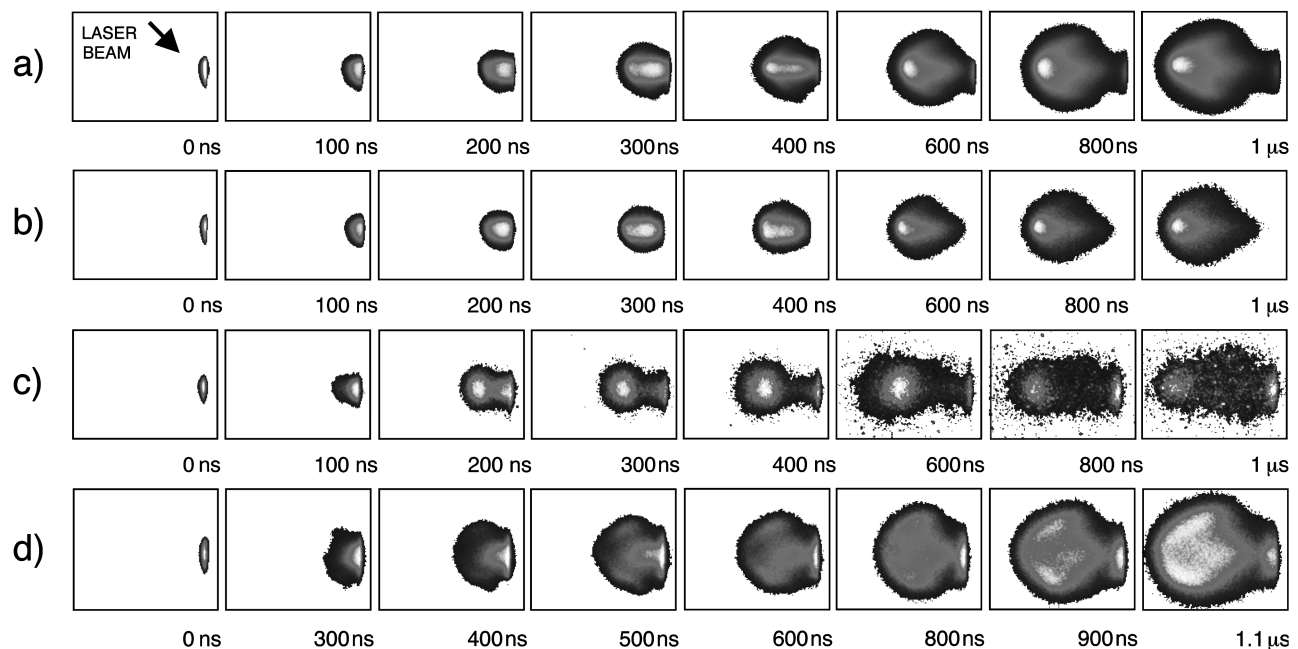


FIG. 1. Series of images obtained from the plume generated by KrF laser ablation of a HA target in a water atmosphere for several delay times corresponding to: (a) total emission, (b) emission from neutral Ca (520 nm), (c) emission from neutral O (777 nm), and (d) emission from calcium oxide (600 nm). The MCP voltage is different for each image and in the gray scale, the darker levels correspond to the lower levels of intensity and the brighter ones to the higher ones.

tween the CCD and the imaging optics of the camera in order to acquire images of the evolution of single emissive species in the plume and, thus, to map their distribution along the plasma.

III. RESULTS AND DISCUSSION

Images of the expansion of the HA ablation plume generated by KrF laser irradiation under a 0.1 mbar water atmosphere for delay times after the laser pulse up to $1.1 \mu\text{s}$ are shown in Fig. 1(a). They show two emissive components reported in detail elsewhere.^{8,12} The first has a hemispherical expansion front and corresponds to the development of a shock wave due to the confinement of some of the ablated species in the plume leading edge by the background atmosphere. The second, almost indistinguishable, appears as a small tenuous spot close to the target surface which is believed to arise from backscattering of a fraction of the species in the plume.¹³ The position versus time of the expansion front of the first component in the plume, assumed as 10% of the intensity maximum,⁸ is shown in Fig. 2(a). A potential expression $R = At^\alpha$ has been chosen to fit the experimental points, where R is the position of the leading edge, t is the time, and A and α are the parameters of the fit. The parameters of the fit were $A = 1.3 \text{ cm}/\mu\text{s}^\alpha$ and $\alpha = 0.6$. Although the dynamics of a spherical shock wave is described by a potential expression like the former one with $\alpha = 0.4$,¹⁴ the fit carried out here does not correspond to such behavior since it corresponds to several experimental points prior to the whole development of the shock structure. The position of the leading edge of the second component of the plume versus time is also shown in Fig. 2(a). The experimental points are well aligned, which means that the expansion took place at constant velocity. This was calculated from the

plot and found to be $2.4 \times 10^3 \text{ m/s}$, a result very similar to the $2.9 \times 10^3 \text{ m/s}$ that corresponds to the case of ablation in vacuum under identical conditions.¹¹

Images recorded through the 520 nm filter are shown in Fig. 1(b). This filter intercepts the emission line at 519 nm of neutral calcium^{10–12} and the images as obtained reveal the spatial distribution of the excited state of this emissive spe-

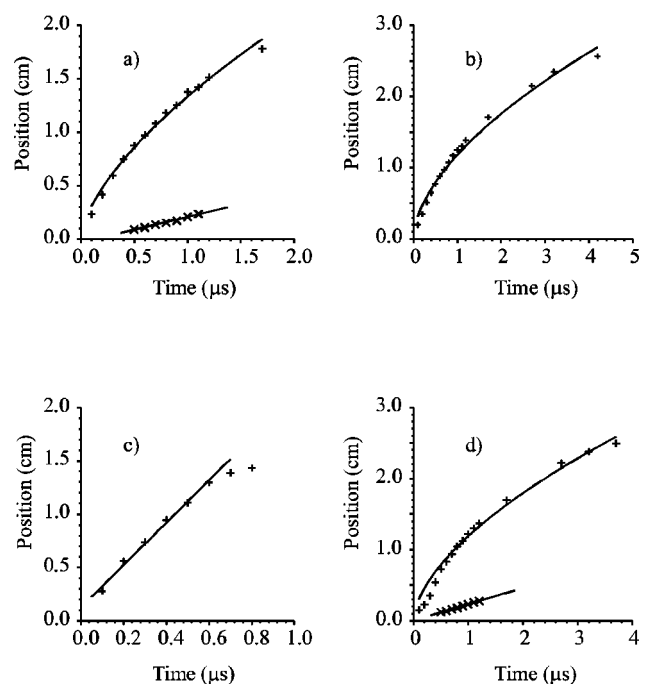


FIG. 2. Plots of the position vs time of the leading edge of the first (+) and second component (x) corresponding to: (a) total emission, (b) emission from neutral Ca (520 nm), (c) emission from neutral O (777 nm), and (d) emission from calcium oxide (600 nm).

cies along the plume. The intensity pattern is almost the same as in Fig. 1(a), corresponding to the total emission, excepting emission from the second component of the plume, absent in Fig. 1(b), as observed under vacuum.^{9–11} The position of the leading edge of the emission pattern of Ca versus time is shown in Fig. 2(b). The parameters of the fit were found to be $A = 1.2$ and $\alpha = 0.6$, values very close to the ones corresponding to the total emission of the plume. Therefore, calcium neutrals remain confined by the background atmosphere in the shock front of the plume.

Images obtained with the aid of a 780 nm filter are shown in Fig. 1(c). They correspond to emission from neutral oxygen since they intercept the triplet at 777 nm. These images present several important differences with respect to the ones from Ca. The intensity maximum does not appear as close to the leading edge of the first component as it did in the case of Ca. This reveals that the confinement of oxygen by the background atmosphere is weaker than in the preceding case. If the series in Figs. 1(b) and 1(c) are compared, the coincidence in the position of the maxima of Ca and O patterns can be noticed. This means that the confinement of both species holds in the same area, but oxygen diffuses beyond that front, inside the water atmosphere, and calcium does not. It can be easily understood since an oxygen atom is considerably lighter and smaller than a calcium one, which enhances a higher level of diffusion of the first one inside the vapor. Furthermore, there is emission from neutral oxygen in the area close to the target surface, in the second component of the plume, in contrast to what happened with Ca and in the same way as in vacuum.¹¹ Images of O look darker than those of Ca and they are full of “dark spots.” This is due to the low intensity of the triplet at 777 nm.¹¹ The dynamics of the expansion of the emission pattern of O has been analyzed from the plots of the position of the leading edge versus time [Fig. 2(c)]. The experimental points are quite well aligned for delay times before 700 ns. In this case, a straight line is a better fit than a potential expression. The fit results in a velocity of expansion for the leading edge of 2.0×10^4 m/s. Under the same fluence conditions in vacuum, the velocity of the O pattern was 1.8×10^4 m/s.¹¹ This indicates that a portion of the oxygen component diffuses inside the vapor without interacting with it. In the second component of the plume, the signal-to-noise ratio is too low to determine the position of the expansion front of the oxygen close to the target surface and, thus, to analyze its dynamics.

Images recorded through a 600 nm bandpass filter are shown in Fig. 1(d). This filter intercepts a 10-nm-wide portion of the second emission band of the orange system of calcium oxide (Ca_xO_y).^{10–12} The analysis of this species is especially interesting since the recorded spectra have revealed that the intensity of emission from the orange system is much higher in a water atmosphere¹² than in vacuum.¹¹ A spherical front develops after 400 ns but it does not correspond to an intensity maximum, that is, to a shock wave. At any time, the maximum remains close to the target, in the second component of the plume, in contrast to what happened with calcium and oxygen [Figs. 1(b) and 1(c)]. After 600–700 ns the intensity distribution changes and some local maxima appear along the plume surface (light areas in the

images). They become very intense after 1 μs and finally develop a shock front with the intensity maximum in the leading edge for delay times of about 1.2 μs . Therefore, it seems that the strong emission in the front does not arise from the confinement of calcium oxide in this region by interaction with the background atmosphere, as suggested previously,¹² since such collisional confinement appears earlier in Ca images. So, the hypothesis of chemical reactions in the plume front¹² seems to be more probable, but only more accurate analysis can confirm this. Regarding the analysis of the dynamics of the emissive calcium oxide, plots of the position versus time of the leading edge of the emission pattern corresponding to Ca_xO_y are shown in Fig. 2(d). The result of the potential fitting is $A = 1.2 \text{ cm}/\mu\text{s}^\alpha$ and $\alpha = 0.6$, identical to the case of Ca. The fitting corresponds to all the experimental points but the shock wave did not develop until about 1.2 μs , a longer delay than that corresponding to Ca. Therefore, although the behavior of each species is different, their dynamics are the same. This suggests that calcium oxide radicals arise directly from calcium atoms, possibly through synthesis and, thus, they follow the same expansion dynamics as the precursor species. Similar processes leading to the formation of molecular radicals in the ablation plume have been described for other materials.^{15,16} Finally, the expansion of the Ca_xO_y component close to the target surface was also studied. From the plots in Fig. 2(d), it appears that the expansion takes place at a constant velocity of 2.3×10^3 m/s, similar to that of the second component of the plume. Therefore, the dynamics and composition of the second component in the plume is the same in vacuum and in a background atmosphere.¹¹ This behavior could be understood in terms of a shielding effect: Species in the second component would not interact with the background gas since they would be shielded from the water atmosphere by species in the first one.

In order to establish whether the reaction in the plume leading to Ca_xO_y involve the atmosphere, ablation experiments were repeated under 0.1 mbar Ne. The atomic mass of Ne is very close to the molecular mass of water, which would result in the same mechanical effects in the development of the shock front, but it is a nonreactive gas. Images recorded without and through the available filters at a 0.1 mbar Ne atmosphere have been depicted in Fig. 3. Pictures corresponding to the total emission of the plume and to the Ca and O emission [Figs. 1(a)–1(c)] are similar to those obtained in water vapor. Only some differences in the shape and intensity hold and thus, it can be inferred that the mechanical effect of Ne on the plume expansion is similar to that of water. On the other hand, images corresponding to Ca_xO_y emission are different. The complex behavior in the first plume component observed in water vapor is not reproduced in the Ne atmosphere. In this case, only a very low contribution to intensity in the first component is present for delay times shorter than 800 ns. Otherwise, the contribution to the second plume component of that species remains unchanged with respect to the case of a water atmosphere. Therefore, considering that the confinement effect has been found to be the same in water vapor and Ne, it is evident that the chemical reactions assumed before take place between

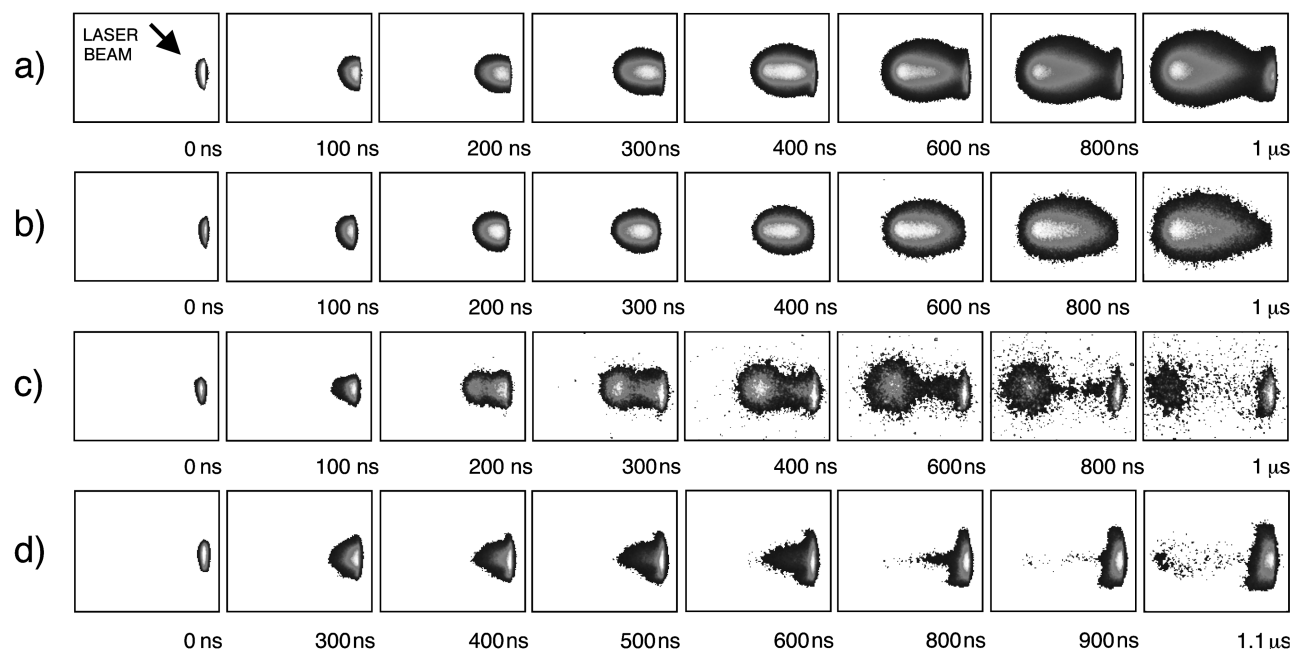


FIG. 3. Series of images obtained from the plume generated by KrF laser ablation of a HA target in a Ne atmosphere for several delay times corresponding to: (a) total emission, (b) emission from neutral Ca (520 nm), (c) emission from neutral O (777 nm), and (d) emission from calcium oxide (600 nm). The MCP voltage is different for each image and in the gray scale, the darker levels correspond to the lower levels of intensity and the brighter ones to the higher ones.

the species in the plume and the water atmosphere, leading to the formation of excited calcium oxide in the first plume component. The next step in this analysis would be addressed to clarify the role and importance of these molecular radicals in the thin film synthesis and only further and more complex experiments could give a definitive answer to these questions.

IV. CONCLUSION

The expansion dynamics of the HA laser ablation plume in a 0.1 mbar water atmosphere has been analyzed by means of fast intensified CCD imaging. The presence of two emissive components has been identified for delay times up to 1.1 μ s. It has been found that the first component develops a shock wave due to the confinement of the species in the leading edge of the plume, whereas the dynamics of the second component has been found to be the same as under high vacuum conditions.

The dynamics and distribution along the plume of some emissive single species (neutral calcium, neutral oxygen, and calcium oxide radicals) has been studied by the same technique with the aid of bandpass interferometric filters. This study has revealed a strong confinement of calcium atoms in the front, leading to the formation of the shock wave, and the absence of these atoms as emissive species in the second component of the plume.

Regarding the oxygen population, there are important contributions to emission in both components of the plume. It has been found that oxygen atoms in the first component are partially confined in the front, like calcium atoms, but the confinement is not so strong as in the preceding case and marked diffusion of neutral oxygen is detected. The differences in the degree of confinement between calcium and

oxygen have been attributed to differences in size and mass of their atoms. The low signal-to-noise ratio prevented analysis of contribution to the second component of the plume.

Emission from calcium oxide radicals has been identified in both components of the plume. The intensity pattern corresponding to the contribution to the first component has been found to follow a complex evolution in time. The detailed analysis of its dynamics has revealed chemical reactions in that region leading to the formation of those molecular species and their further confinement in the shock front. Once more, the contribution to the second component has been found to be the same as in the vacuum case, suggesting shielding in the motion of the second component due to the first one.

Finally, the comparison of HA ablation in a water atmosphere with ablation in a Ne atmosphere has revealed that the processes leading to the formation of calcium oxide radicals arise from chemical reactions between the first component of the plume and the background water atmosphere and not among the species confined in the high density shock front.

ACKNOWLEDGMENTS

This work has been supported by CICYT of the Spanish Government (Project No. MAT94-0264) and DGR of the Catalan Government.

¹P. Baeri, L. Torrisi, N. Marino, and G. Foti, *Appl. Surf. Sci.* **54**, 210 (1992).

²C. M. Cotell, D. B. Chrisey, K. S. Grabowski, and J. A. Sprague, *J. Biomater. Appl.* **3**, 87 (1992).

³G. Sardin, M. Varela, and J. L. Morenza in *Hydroxyapatite and Related Materials*, edited by P. W. Brown and B. Constantz (Chemical Rubber, Boca Raton, 1994), p. 225.

⁴V. N. Bagratashvili, E. N. Antonov, E. N. Sobol, V. K. Popov, and S. M. Howdle, *Appl. Phys. Lett.* **66**, 2451 (1995).

- ⁵M. Jelínek *et al.*, *Laser Phys.* **6**, 144 (1996).
- ⁶J. M. Fernández-Pradas, G. Sardin, L. Clèries, P. Serra, C. Ferrater, and J. L. Morenza, *Thin Solid Films* **317**, 394 (1998).
- ⁷F. García, J. L. Arias, B. Mayor, J. Pou, I. Rehman, J. Knowles, S. Best, B. León, M. Pérez-Amor, and W. Bonfield, *J. Biomed. Mater. Res.* **43**, 69 (1998).
- ⁸P. Serra, J. Palau, M. Varela, J. Esteve, and J. L. Morenza, *J. Mater. Res.* **10**, 473 (1995).
- ⁹P. Serra, J. M. Fernández-Pradas, G. Sardin, and J. L. Morenza, *Appl. Surf. Sci.* **109/110**, 384 (1997).
- ¹⁰P. Serra and J. L. Morenza, *J. Mater. Res.* **13**, 1132 (1998).
- ¹¹P. Serra and J. L. Morenza, *Appl. Surf. Sci.* **127–129**, 662 (1998).
- ¹²P. Serra and J. L. Morenza, *Appl. Phys. A: Mater. Sci. Process.* **67**, 289 (1998).
- ¹³P. Serra and J. L. Morenza, *Thin Solid Films* **335**, 43 (1998).
- ¹⁴Y. B. Zel'dovich and P. Raizer, *Physics of Shock Waves and High Temperature Hydrodynamic Phenomena* (Academic, New York, 1966), Vol. 1, p. 94.
- ¹⁵C. Girault, D. Damiani, J. Aubreton, and A. Catherinot, *Appl. Phys. Lett.* **55**, 182 (1989).
- ¹⁶D. B. Geohegan and A. A. Puretzky, *Mater. Res. Soc. Symp. Proc.* **397**, 55 (1996).